Phase transitions on fractals. III. Infinitely ramified lattices

1984 J. Phys. A: Math. Gen. 17 1277

(http://iopscience.iop.org/0305-4470/17/6/024)

J. Phys. A: Math. Gen. **17** (1984) 1277–1289. Printed in Great Britain

Phase transitions on fractals: III. Infinitely ramified lattices

Yeval Gefen†, Amnon Aharony‡ and Benoit B Mandelbrot§

† Institute for Theoretical Physics, University of California, Santa Barbara, CA 93106, USA
† Department of Physics and Astronomy, Tel Aviv University, Israel
§ IBM T J Watson Research Center, Yorktown Heights, New York 10598, USA.

Received 18 August 1983

Abstract. In the first two papers of this series we considered self-similar fractal lattices with a finite order of ramification R. In the present paper we study physical models defined on a family of fractals with $R=\infty$. In order to characterise the geometry of these systems, we need the connectivity Q and the lacunarity L, in addition to the fractal dimensionality D. It is found that discrete-symmetry spin models on these lattices undergo a phase transition at $T_c>0$. An approximate renormalisation group scheme is constructed and used to find the dependence of T_c and the critical exponents on the geometrical factors. We also solve the problem of resistor networks on these fractals, and discuss its consequences concerning spin models with continuous symmetry.

1. Introduction

In two previous papers (Gefen *et al* 1983a, 1984—hereafter referred as I and II) we have analysed the critical behaviour of various spin systems on certain self-similar lattices with non-integer fractal dimensionalities D and a finite order of ramification, R. None of these systems exhibited phase transitions at finite temperatures. In this paper we complete the series by considering the family of Sierpinski carpets, for which $R=\infty$. The geometrical characterisation of such systems requires additional parameters, e.g. the connectivity, Q, and the lacunarity, L. We find that critical exponents depend on these parameters, thus generalising the concept of universality.

The outline of the paper is as follows: the various geometrical parameters which are needed are introduced in § 2. Section 3 is devoted to an analysis of Ising models on these fractals. We construct an approximate renormalisation-group scheme, find how the critical temperature and the critical exponents vary with the geometrical factors, and describe the flow diagrams in the Hamiltonian space. In § 4 we study the scaling of resistor networks defined on these fractals. The results are used to derive the low temperature properties of spin systems with $n\geqslant 2$ components. Section 5 contains our conclusions.

2. Geometry of the Sierpinski carpets

The fractal lattices studied in this paper are called Sierpinski *carpets* (Mandelbrot 1977, 1982, ch 14, Gefen *et al* 1980). They are constructed in the following way: we start with a square of unit area. This square is subdivided into b^2 subsquares, out

0305-4470/84/061277+13$02.25

of which $\tilde{n}$ squares are cut out. The procedure is then repeated for the smaller squares, and iterated until one reaches the 'microscopic' length scale. The resulting geometrical shape is self-similar on all the intermediate length scales. In the following we shall be interested in cases in which $\tilde{n} = l^2$ (l being an integer), and the $\tilde{n}$ squares are eliminated in a symmetric fashion. We first study the case in which the l^2 squares form one large island at the centre of each larger square. Such a case, with $b = 7$ and $l = 3$, is shown in figure 1(*a*).

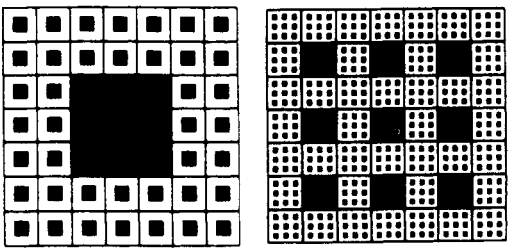

(*a*) (*b*)

Figure 1. Two stages of Sierpinski carpets with $R = \infty$, $b = 7$, $l = 3$, $D = 1.8957$ and $Q \simeq 0.7124$. (*a*) $L \simeq 3.924$, (*b*) $L \simeq 0.9984$.

The fractal dimensionality, D, is generally defined so that b^D is equal to the number of new smaller units (Mandelbrot 1977, 1982). In our case, $b^D = b^2 - \tilde{n} = b^2 - l^2$, and we have (Mandelbrot 1977, 1982, Gefen *et al* 1980)

$$D = \ln(b^2 - l^2)/\ln b. \tag{2.1}$$

In the two examples shown in figure 1 we have $b = 7$ and $l = 3$, so that $D = \ln 40/\ln 7 \simeq 1.8957$. More examples are listed in table 1. Letting b have very large values, and varying l, one may construct carpets with D arbitrarily close to any value between 1 and 2 (Gefen *et al* 1983b). Our fractals are embedded in a two-dimensional Euclidean space ($d = 2$) and have the topological dimensionality $D_T = 1$. Thus the general relation $d \geqslant D \geqslant d_T$ (Mandelbrot 1977, 1982) is satisfied. The generalisation to $d > 2$ is straightforward.

The order of ramification, R, at a point P, is equal to the number of significant bonds which one must cut in order to isolate an arbitrarily large bounded set of points connected to P (see Mandelbrot 1982, ch 14 and I, II). For the carpets, this number grows as a power of the size of this bounded set, so that $R = \infty$. Instead, we thus consider the fractal dimensionalities of the 'surfaces' of the isolated bounded sets, $\{D'\}$. *The connectivity*, Q, is defined as the smallest value of D', $Q = \min\{D'\}$†. For our two-dimensional carpets, the 'surface' of an isolated set has the Euclidean dimensionality of a line, $d = 1$. In our case, with $\tilde{n} = l^2$, boxes whose sides are vertical and horizontal straight lines that pass through l small squares have the smallest surface fractal dimensionality, so that

$$Q = \ln(b - l)/\ln b. \tag{2.2}$$

In the examples of figure 1, $Q = \ln 4/\ln 7 \simeq 0.7124$. (See also table 1). Note that in

† Another treatment of the connectivity is that of Dhar (1980). However, his 'connectivity', c, is related to Q by $c = (1 - Q/D)^{-1}$. It has also been pointed out by Suzuki (1983), that an alternative definition of the connectivity, $\tilde{Q} \equiv \min\{D''\}$, where D'' is the dimensionality of a 'cut' that separates an infinite subset from the original one, may yield another value. An example is the Cayley tree, for which $Q = \infty$ whereas $\tilde{Q} = 0$.

Table 1. Results for the Ising model on carpets with a central cutout.

b	l	D	Q	τ_E^*	$\lambda_{E,\tau}$	λ_{E,τ_w}	$(\tau_F, \tau_{w,F})$	$\lambda_{F,1}$	$\lambda_{F,2}$	τ_c
3	1	≃1.893	≃0.631	≃0.120	≃0.5621	≃0.4119	(≃0.6995, ≃0.0156)	≃0.2237	≃−0.797	≃0.311
7	5	≃1.633	≃0.356	≃0.021	≃0.3483	≃0.2926	(1, ≃0.66)	≃0.34	≃−0.920	≃0.665
11	9	≃1.538	≃0.289	≃0.0083	≃0.2870	≃0.2544	(1, ≃0.80)	≃0.28	≃−0.940	≃0.80
15	13	≃1.486	≃0.256	≃0.0045	≃0.2546	≃0.2329	(1, ≃0.86)	≃0.25	≃−0.963	≃0.86
7	3	≃1.896	≃0.712	≃0.087	≃0.594	≃0.445	(≃0.261, ≃0.013)	≃0.524	≃−1.436	≃0.194
11	7	≃1.784	≃0.578	≃0.045	≃0.5116	≃0.3889	(≃0.44, ≃0.0033)	≃0.418	≃−1.239	≃0.271
15	11	≃1.716	≃0.512	≃0.029	≃0.4657	≃0.3601	(≃0.53, ≃0.0010)	≃0.383	≃−1.468	≃0.333
11	3	≃1.968	≃0.867	≃0.085	≃0.6480	≃0.5108	(≃0.122, ≃0.009 17)	≃0.650	≃−2.049	≃0.113
15	7	≃1.329	≃0.768	≃0.058	≃0.5984	≃0.4690	(≃0.148, ≃0.001 74)	≃0.558	≃−1.953	≃0.123
31	29	≃1.394	≃0.202	≃0.0010	≃0.2027	≃0.1927	(1, ≃0.934)	≃0.198	≃−0.9866	≃0.93
31	23	≃1.767	≃0.606	≃0.024	≃0.5086	≃0.3980	(≃0.244, ≃$3 \cdot 10^{-5}$)	≃0.477	†	≃0.191
31	11	≃1.961	≃0.872	≃0.041	≃0.6105	≃0.5162	(≃0, ≃0)	†	†	≃0.06
31	3	≃1.997	≃0.970	≃0.047	≃0.6370	≃0.5608	(≃0, ≃0)	†	†	≃0.049

† Impossible to determine accurately.

general $d-1 \geqslant D' \geqslant Q$. The cutting dimensionality is almost surely equal to $(D-1)$ if the cutting line is drawn at random (Mandelbrot 1982, p 135).

Another geometrical characteristic of these fractals is the *lacunarity* L, (Mandelbrot 1979, Gefen *et al* 1980, 1983b). We can construct two Sierpinski carpets with the same D and Q, for which the eliminated squares are scattered differently. Such an example is presented in figures 1(a) and 1(b). The first one has a larger lacunarity, reflecting the fact that it is less homogeneous. Lacunarity measures the extent of the failure of a fractal to be translationally invariant, or the fluctuations around the 'mass distribution law' $M \sim r^D$ where M is the 'mass' (the number of sites) of a part of the system whose linear size is r. In the present study we evaluate an approximate expression for L. We consider all the n square subarrays $l \times l$ cells in an array of $b \times b$ cells. For each of these $l \times l$ 'coverings', i, we count the number of non-eliminated subsquares, n_i. The lacunarity is approximated by the mean square deviation of n_i from its average,

$$L \equiv \frac{1}{n} \sum_i (n_i - \bar{n})^2, \tag{2.3}$$

where $\bar{n} = \Sigma_i n_i / n$. For lattice in figure 1(a), one has four 'coverings' which contain one eliminated subsquare, eight 'coverings' containing two eliminated subsquares, four with three eliminations, etc. In this case $\bar{n} = 5.75$ and $L = 3.9424$. For the lattice in figure 1(b), with the same D and Q, $L = 0.9984$. Obviously, the lattice in figure 1(b) is much more homogeneous. For translationally invariant lattices expression (2.3) yields $L = 0$. We have recently shown that the properties of the carpets approach those of hypercubic lattices, with the same non-integer dimensionality, in the limit $L \to 0$. This limit may be obtained by letting $b \to \infty$ and by scattering the eliminated squares as uniformly as possible (Gefen *et al* 1983b).

It should be noted that, in general, the properties of a carpet with fractal dimensionality D differ from those of a hypercubic lattice with the same dimensionality. One typical characteristic of the latter is the number of bonds per site, which is equal to D. In appendix 1 we calculate the average number of bonds per site, for our carpets, and show that this number differs from D. The differences depend on the lacunarity. We expect these differences to disappear in the limit $L \to 0$ (Gefen *et al* 1983b).

Finally, it is interesting to note (Mandelbrot 1982, p 135) that the asymmetric case of $b = 2$, $l = 1$ (one subsquare is eliminated in a corner) is topologically equivalent to the Sierpinski gasket in two dimensions (see II), which can be directly related to the percolation problem (Gefen *et al* 1981).

3. Results for Ising models

We now place a spin variable on each lattice site of the microscopic lattice (obtained after iterating our decorating procedure down to a 'microscopic' length scale and stopping there). Spins are placed on all the lattice sites, including those which border the eliminated areas. The Hamiltonian of the Ising model is now written as

$$\mathcal{H} = -J \sum_{\langle ij \rangle} S_i S_j, \tag{3.1}$$

where $\langle ij \rangle$ denotes a nearest-neighbour bond (on the microscopic lattice!). We believe that, unlike the cases with $R < \infty$, discussed in I and II, all fractals with $R = \infty$ have

phase transitions at *finite temperatures*. There are several ways of verifying this general statement. In our earlier work (Gefen *et al* 1980) we presented a low temperature renormalisation group which implies the existence of an unstable fixed point at finite temperature (representing the critical point). In this section we summarise the results of an approximate bond-moving Migdal–Kadanoff real space renormalisation-group study (Migdal 1975, Kadanoff 1976), yielding the same result (as well as quantitative estimates of critical exponents). Since this approximation is expected to be very accurate at low temperatures, where it predicts a stable zero temperature fixed point, it supports our belief that one will always find a transition at a finite temperature.

The iteration of the renormalisation-group transformation generates two basic exchange variables. We denote the 'coupling' via a bond which separates between two non-eliminated subsquares by $K = J/k_B T$ (k_B is the Boltzmann constant and T is the temperature), and that of a bond which borders an eliminated subsquare by $K_w = J_w/k_B T$. The renormalisation procedure is composed of two steps: we first move all the bonds within a dedecorated (large) square to its perimeter (parallel to themselves), and then decimate the resulting (one-dimensional) perimeter bonds (Kadanoff 1976). Figures 2 and 3 exhibit the construction of K' and K'_w, respectively, for the case $b = 3$,

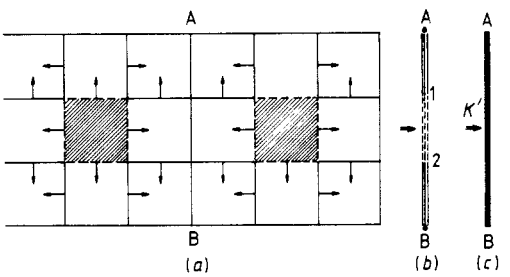

Figure 2. Three steps in obtaining the renormalised K' between sites A and B for the case $b = 3$ and $l = 1$. Full lines denote K whereas broken lines stand for K_w. (*a*) Directions of bond moving. (*b*)Bonds between A and B before decimating. (*c*) Final result after decimating over the degrees of freedom 1 and 2.

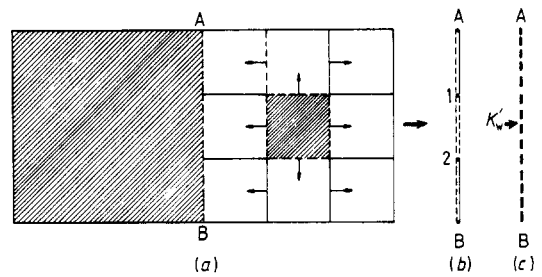

Figure 3. Same as figure 2, for K'_w.

$l = 1$. The small arrows indicate the directions in which the bonds are moved. For a renormalised bond between two non-eliminated large squares (AB in figure 2), the first step ends up with three bonds in series, with coupling strengths $3K$, $K + 2K_w$ and $3K$, respectively (figure 2(*b*)). The decimation of the two intermediate spins in figure 2(*b*) then yields the renormalised bond K' (figure 2(c)), with

$$\tanh K' = \tanh^2 3K \tanh(K + 2K_w). \tag{3.2a}$$

Similarly, the construction in figure 3 explains how one obtains the renormalised coupling K'_w,

$$\tanh K'_w = \tanh^2(K + K_w) \tanh 2K_w. \tag{3.2b}$$

A generalisation of this example to the case in which a single large square, of size $l \times l$, is eliminated in the centre of each larger square (figure 1(*a*)) yields

(Gefen *et al* 1980)

$$\tanh K' = \tanh^{l}[(b-l-1)K + 2K_w] \tanh^{b-l}(bK), \tag{3.3a}$$

$$\tanh K'_w = \tanh^{l}[\tfrac{1}{2}(b-l-2)K + 2K_w] \tanh^{b-l}[\tfrac{1}{2}(b-1)K + K_w]. \tag{3.3b}$$

Notice that within the approximation described above, the recursion relations close within the two-dimensional parameter-space, (K, K_w). For $l = 0$ we recover the known $d = 2$ results (Migdal 1975, Kadanoff 1976).

For convenience we shall represent our results using the variables

$$\tau = \tanh K, \qquad \tau_w = \tanh K_w. \tag{3.4}$$

Since the $l \times l$ square is placed in the centre of the $b \times b$ square, we have $b \geqslant l+2$. If $b > l+2$ then we find three trivial fixed points,

$$A: (0,0), \qquad B: (0,1), \qquad C: (1,1), \tag{3.5}$$

where the coordinates refer to (τ, τ_w). For $b = l+2$ there exists an additional trivial fixed point,

$$D: (1,0) \qquad (b = l+2). \tag{3.6}$$

Examples of the renormalisation group flows (3.3), in the $\tau - \tau_w$ plane, are shown in figure 4. The point D is a fixed point in figure 4(a) ($b = 3$, $l = 1$) and 4(b) ($b = 7$, $l = 5$), but not in figure 4(c) ($b = 7$, $l = 3$). In all the cases, the point A corresponds to K and

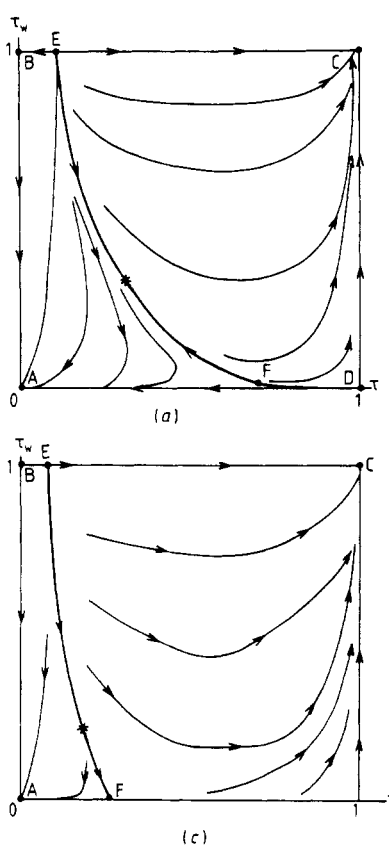

Figure 4. Flow diagrams for Sierpinski carpets with a central cutout. (a) $b = 3$, $l = 1$. (b) $b = 7$, $l = 5$. (c) $b = 7$, $l = 3$. Quantitative data are given in table 1.

K_w being zero, hence this is the infinite temperature (paramagnetic) fixed point. Point B corresponds to $K=0$ and $K_w=\infty$, and describes an anisotropic situation, where the sites on a 'wall' are coupled infinitely strongly. The third point C is the isotropic $T=0$ (ferromagnetic) point. The point D is also a zero temperature point, but with non-interacting 'wall sites' (free ends). This fixed point, and the whole line $K_w=0$, represent systems like the one shown in figure 5 ($b=3$, $l=1$ with no bonds on the boundaries of the eliminated squares).

We next discuss flows along special axes. Starting at a point $(0, \tau_w)$ on the τ_w axis ($\tau=0$), the flow stays on this axis, going from B to A. Flows which start on the line $\tau_w=1$ also stay on it. We can expand (3.3) near B and C (see appendix 2), and find that there are flows along the line $\tau_w=1$ towards B and C; hence there is another fixed point on the $\tau_w=1$ line, unstable in the direction of this axis. We denote this point by E. Now we have to distinguish between the cases $b=l+2$ and $b>l+2$.

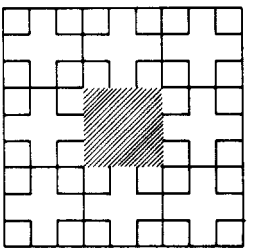

Figure 5. Two stages of Sierpinski carpet ($b=3$, $l=1$) with free ends ($\tau_w=0$).

We start with $b=l+2$. In this case, D is a fixed point, and flows which start on the τ axis ($\tau_w=0$) stay on it, flowing from D to A. We recall that the points along this line correspond to configurations with free ends. For, the case $b=l+2$, setting $\tau_w=0$ lowers the order of ramification from $R=\infty$ to a finite value, i.e., $R=2$, 3 or 4, without changing the fractal dimensionality (cf figure 5). Thus, we should obtain a quasi one-dimensional flow (as considered in I, II) along the $\tau_w=0$ axis. For the $b>l+2$ case R is infinite and the situation is completely different.

We next consider the line $\tau=1$. Again, flows remain on this line. Expansions of (3.3) near C and D reveal that these points are stable along this line, so that there must exist an additional unstable fixed point with $\tau=1$. We denote this point by F. It turns out that the case $b=3$, $l=1$ is special, and we treat it separately below.

We now turn to the case $b>l+2$. As mentioned above, D is no longer a fixed point. Starting on the τ axis ($\tau_w=0$), flows leave this axis and develop finite values of τ_w. All the points on the line $\tau=1$ (including the point D) flow (in one iteration) to the point C. The second non-trivial fixed point F is now removed from the line $\tau=1$, and appears near the τ-axis.

The stability analysis in the vicinity of each fixed point is described in detail in appendix 2. In addition to that analysis, we iterated the recursion relations numerically, and identified the locations of, and the exponents near, the fixed points E and F. The numerical results are summarised in table 1. For each pair of b and l, the table lists D, Q, τ_E^* and the exponents near E, the coordinates of F and the exponents near F, and the critical value τ_c (at which the critical line EF crosses the diagonal $\tau_c=\tau=\tau_w$).

We find three typical flow diagrams. Figure 4(*a*) shows the special case $b=3$, $l=1$, which differs from all the cases with $b=l+2>3$. The latter cases are represented by

figure 4(*b*) ($b = l+2 = 7$). Figure 4(*c*) shows a typical flow diagram for $b > l+2$ ($b = 7$, $l = 3$). In all the cases the bold line EF represents the critical line, separating the disordered phase (flows to A) from the ordered one (flows to C). The critical point is represented by the fixed point F, and the thermal exponent ν is equal to $1/\lambda_{F,1}$.

Notice the monotonic variation of the exponents (and the fixed points coordinates) as we change D or Q, but keep some variable (such as b or l) constant. A notable exception is the $b = l+2 = 3$ case, where, for example, the exponent $\lambda_{F,1}$ does not obey the monotonic decrease with D. This case is also special in the topology of the flow diagram, see figure 4(*a*). Except for this special case, the exponent ν increases as D (and Q) are decreased. This is similar to the known hypercubic lattices, for which ν decreases monotonically from ∞ at $d = 1$ to $\frac{1}{2}$ at $d = 4$.

As was mentioned above we can construct various carpets where we vary L and keep D, R, Q, etc constant. We present here relations analogous to (3.3) for the case of 'scattered lacunarity' (cf figure 1(*b*)), where the eliminated subsquares are scattered symmetrically and do not touch each other. As an example, we consider the case $l = \frac{1}{2}(b-1)$. The recursion relations are

$$\begin{aligned} \tanh K' &= \tanh^{b-l}(bK)\tanh^{l}[K+(b-1)K_w], \\ \tanh K'_w &= \tanh^{b-l}(lK+K_w)\tanh^{l}[(l+1)K_w]. \end{aligned} \tag{3.7}$$

An analysis similar to that presented in appendix 2, together with a numerical analysis, yield figure 6. Qualitatively, the results are similar to those of figure 4. Quantitatively, the details are very different. Although figure 6 was calculated for $b = 7$ and $l = 3$, which have the same values as figure 4(*c*) (and therefore the same values of D and Q), the fixed point F is now at $(1, \simeq 0.1448)$, τ_c is now increased to $\simeq 0.245$ (instead of $\simeq 0.194$), and the exponents at F are $\simeq 0.460$, $\simeq -0.335$ (instead of $\simeq 0.524$, $\simeq -1.436$). The point E and its exponents remain unchanged. We conclude that at fixed D and Q, ν increases with decreasing lacunarity. This simple example indicates that lacunarity affects the universal behaviour. The topic deserves full study.

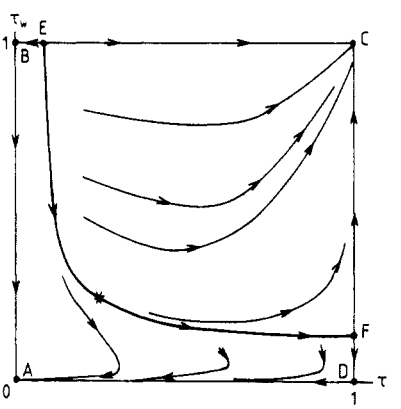

Figure 6. Flow diagrams for Sierpinski carpet with scattered cutouts, $b = 7$, $l = 3$ (cf figure 1(*b*)).

4. Resistor networks

In this section we study the scaling of the resistivity of resistor networks which are put on Sierpinski carpets. We use the same approximate renormalisation group scheme described in § 3. We put resistors R_w on bonds which border eliminated squares, and

resistors R elsewhere. A renormalisation step includes moving the resistors to the perimeter of each large square, adding the resistivities of parallel resistors, then summing the resulting resistivities in series, and obtaining equivalent resistors for the renormalised system.

For systems with one symmetric central cutout we obtain the following recursion relations

$$R' = \frac{(b^2+l^2-lb-2b+2l)RR_w+3(b-l)R^2}{b[R_w(b-l-2)+3R]},$$
$$R'_w = \frac{RR_w^2 2(b^2+l^2-lb-2b+l)+4(2b-l)R^2R_w}{[(b-1)R_w+2R][(b-l-2)R_w+4R]}. \tag{4.1}$$

Notice that this method is *exact* for translationally invariant two-dimensional lattices, no matter what b is.

We now study the flows in the (R, R_w) space. One should recall that due to the fact that resistivities rather than conductivities are used, the analogue of the point $(0,0)$ of the previous section is now (∞,∞), etc. We start with some limiting cases. $R=0$: In one iteration all the flows reach the point $(0,0)$. $R_w=0$: In this case $R'_w=0$, and $R'=[(b-l)/b]R$. Thus we flow on the $R_w=0$ axis towards $(0,0)$. $R=\infty$: We have $R'=\infty$, $R'_w=(b-\frac{1}{2}l)R_w>R_w$, and we flow towards (∞,∞). $R_w=\infty$: We obtain $R'=[(b-l)/b+l/(b-l-2)]R>R$, and $R'_w=[2(b^2+l^2-lb-2b+l)/(b-1)(b-l-2)]R>R$. $R=R_w$: We have $R'=R[(b-l)(b-l+1)+lb]/b(b-l+1)\geq R$, with equality for $l=1$, and $R'_w=R(2b^2+2l^2+2lb+4b-2l)/(b+1)(b-l+2)>R$.

It is useful to consider the recursion relation for the ratio $a=R_w/R$,

$$a'=ab\{[2(b^2+l^2-lb-2b+l)a+4(2b-l)][(b-l-2)a+3]\}/$$
$$\times\{[(b^2+l^2-lb-2b+2l)a+3(b-l)][(b-1)a+2][(b-l-2)a+4]\}. \tag{4.2}$$

It is easy to see that for $a\ll 1$ one has

$$a'\simeq[(2b-l)b]/(2b-2l)]a, \tag{4.3}$$

i.e. $a'>a$. Similarly, if $a\gg 1$ then after one iteration one has

$$a'\simeq 2b(b^2+l^2-lb-2b+l)/[(b-1)(b^2+l^2-lb-2b+2l)], \tag{4.4}$$

so that a' becomes of order unity. In general, a will flow to a fixed point value which is determined by the cubic equation

$$b[2(b^2+l^2-lb-2b+l)a+4(2b-l)][(b-l-2)a+3]$$
$$=[(b^2+l^2-lb-2b+2l)a+3(b-l)][(b-1)a+2][(b-l-2)a+4]. \tag{4.5}$$

This fixed point has the value $a^*=2$ for $b\gg l$ (D close to 2) and the value $a^*=\frac{3}{2}$ for $b=l+2\gg 1$ (D close to one). Additional values of a^* are listed in table 2.

Having reached the fixed ratio a^*, equation (4.1) now yields

$$R' = \frac{(b^2+l^2-lb-2b+2l)a^*+3(b-l)}{b[(b-l-2)a^*+3]}R. \tag{4.6}$$

Writing this in the form

$$R'=b^{\tilde{c}}R, \tag{4.7}$$

Table 2. Results for resistor networks on the carpets.

b	l	a^*	$\tilde{\zeta}$	$2-D$
3	1	1.712	0.194	0.107
5	1	1.922	0.048	0.025
5	3	1.580	0.424	0.277
9	1	1.982	0.0099	0.0057
9	3	1.918	0.085	0.054
9	7	1.525	0.605	0.423

we can identify the exponent $\tilde{\zeta}$. For hypercubic lattices one expects that $\tilde{\zeta}=2-d$. Table 2 also contains a comparison between $\tilde{\zeta}$ and $2-D$. In the limiting cases $b \gg l$ and $b=l+2 \gg 1$ we find that $\tilde{\zeta} \simeq 0$ and $\tilde{\zeta} \simeq 1$, in agreement with $(2-D)$ (see also Gefen *et al* 1983b). For all the cases that we studied $\tilde{\zeta}$ satisfies $\tilde{\zeta} \geqslant 2-D$. Note also that table 2 shows monotone variation of $\tilde{\zeta}$ with l (for a fixed b) and with b (for a fixed l).

It is worth noting that the recursion relations for R are the same as those for $K^{-1}=k_B T/J$ for spin models with continuous symmetry ($n \geqslant 2$ spin components) at low temperature (e.g. José *et al* 1977, Stinchcombe 1979). The exponent corresponds to the exponent determining the stability of the zero temperature fixed point. Since we found that $\tilde{\zeta}>0$, this fixed point is unstable, and there is no long range order. This is to be expected, since we considered only the case $D<2$, and the lower critical dimensionality for such models is equal to two. It would be interesting to study the same problem for $D>2$.

5. Conclusion

In this paper we have discussed a family of self-similar lattices with an infinite order of ramification. We emphasised the importance of this and other geometrical factors and their relevance to the critical behaviour of physical models put on these fractals. Besides contributing to the understanding of thermodynamical systems on fractals, we suggest that these models may be related to real physical systems. Thus, for example, in the limit of K_w approaching zero, some of the models become finitely ramified. These and the models that were described in I and II, may serve as models for percolating clusters and backbones (cf Gefen *et al* 1981). The resistor networks described in § 4 may be relevant to the description of conductor–superconductor mixtures.

Acknowledgments

Two of us (YG and AA) gratefully acknowledge stimulating discussions with B I Halperin, Y Shapir, A N Berker and S Fishman, as well as the hospitality of B I Halperin at Harvard University and of the IBM Thomas J Watson Research Center. This work was supported in part by grants from the Israel Academy of Sciences and Humanities and from the US–Israel Binational Science Foundation. We also thank Y Meir for his help with some of the calculations.

Appendix 1. Average number of bonds per site on the carpet

Consider the carpet with a central cutout (of size $l \times l$, out of a square of size $b \times b$). After k decoration iterations, the number of bonds per site is given by

$$\left(\frac{\text{bonds}}{\text{spins}}\right)_k \equiv A_k = \left(2(b^2-l^2)^k + 2\sum_{n=0}^{k-1} lb(b^2-l^2)^{k-n-1}\right) \Big/ \left((b^2-l^2)^k + \sum_{n=0}^{k-1}[2(lb^n-1)+1](b^2-l^2)^{k-n-1}\right). \tag{A1.1}$$

In the example of figure 1(a) ($b=7$, $l=3$, $D \simeq 1.8957$), we have $A_2 \simeq 1.8913$, $A_3 \simeq 1.8878, \ldots$. For carpets of lower lacunarity, when the eliminated subsquares are scattered (e.g. figure 1(b)), the series yields higher values. The general formula is

$$\left(\frac{\text{bonds}}{\text{spins}}\right)_k \equiv A_k = \left(2(b^2-l^2)^k + 2l^2\sum_{n=0}^{k-1} b^n(b^2-l^2)^{k-n-1}\right) \Big/ \left((b^2-l^2)^k + l^2\sum_{n=0}^{k-1}[2(b^n-1)+1](b^2-l^2)^{k-n-1}\right), \tag{A1.2}$$

and for figure 1(b) we find $A_2 \simeq 1.948$, $A_3 \simeq 1.938, \ldots$.

Since in both cases $D \simeq 1.8957$, it is clear that the series $\{A_k\}$ differs from D. The difference seems to depend on the lacunarity, and may probably serve as an alternative measure of it.

Appendix 2. Analysis of recursion relations

The linear stability of the fixed points of (3.3) is governed by the four derivatives

$$\frac{\partial\tau'}{\partial\tau} = \cosh^2 K\left(\frac{b(b-l)\tanh^{b-l-1}(bK)}{\cosh^2(bK)}\tanh^l[2K_w+(b-l-1K] + \frac{l(b-l-1)\tanh^{b-l}(bK)}{\cosh^2[2K_w+(b-l-1)K]}\tanh^{l-1}[2K_w+(b-l-1)]\right), \tag{A2.1}$$

$$\frac{\partial\tau'}{\partial\tau_w} = \cosh^2 K_w \tanh^{b-l}(bK)\frac{2l\tanh^{l-1}[2K_w+(b-l-1)K]}{\cosh^2[2K_w+(b-l-1)K]}, \tag{A2.2}$$

$$\frac{\partial\tau'_w}{\partial\tau} = \cosh^2 K\left(\frac{(b-l)(b-1)\tanh^{b-l-1}[K_w+\frac{1}{2}(b-1)K]}{2\cosh^2[K_w+\frac{1}{2}(b-1)K]}\tanh^l[2K_w+\tfrac{1}{2}(b-l-2)K] + \frac{l(b-l-2)\tanh^{b-l}[K_w+\frac{1}{2}(b-1)K]}{2\cosh^2[2K_w+\frac{1}{2}(b-l-2]K]}\tanh^{l-1}[2K_w+\tfrac{1}{2}(b-l-2)K]\right), \tag{A2.3}$$

$$\frac{\partial\tau'_w}{\partial\tau_w} = \cosh^2 K_w\left(\frac{(b-l)\tanh^{b-l-1}[K_w+\frac{1}{2}(b-1)K]}{\cosh^2[K_w+\frac{1}{2}(b-1)K]}\tanh^l[2K_w+\tfrac{1}{2}(b-l-2)K] + \frac{2l\tanh^{b-l}[K_w+\frac{1}{2}(b-1)K]}{\cosh^2[2K_w+\frac{1}{2}(b-l-2)K]}\tanh^{l-1}[2K_w+\tfrac{1}{2}(b-l-2)K]\right). \tag{A2.4}$$

All four derivatives vanish at the fixed point A. One must therefore go to higher-order terms. Along the $\tau=0$ direction, the flow of τ_w is given by $\tau'_w = 2^l\tau_w^b$. For

$b-l=2$, the other eigendirection is along the $\tau_w=0$ axis, where we have $\tau'=b^{b-l}\tau^b$. The flow into A is thus rather fast.

At the point B we find $(\partial\tau_w'/\partial\tau_w)=b-l$, with all the other derivatives equal to zero. The flow along the BC axis is described by $\tau'=b^{b-l}\tau^{b-l}$, the instability along the AB axis is governed by the exponent

$$\lambda_B=\ln(b-l)/\ln b. \tag{A2.5}$$

All the derivatives also vanish at the fixed point C. The flow towards C along the CD axis is infinitely fast (a single iteration brings directly to C), while that along the BC axis has $\exp(-2K')\simeq(b-l)\exp(-2bK)$.

In the case $b=l+2$, the first three derivatives near the point D have the values l, 0 and 0. The derivative $(\partial\tau_w'/\partial\tau_w)$ has the value 0 if $l\neq 1$ and 2 if $l=1$. The instability of D along the τ-axis is thus described by the exponent

$$\lambda_D=\ln l/\ln b. \tag{A2.6}$$

For $b=3$, $l=1$, D is also unstable along the line $\tau=1$, with $\tilde{\lambda}_D=\ln 2/\ln b$. For $b=l+2>3$, D is strongly stable in this direction, with $\tau_w'=2^l\tau_w^l$.

Note that λ_D represents the quasi-one-dimensional thermal exponent, $1/\nu$ for the case $\tau_w\equiv 0$ (figure 5). As explained in I, the Ising thermal exponent is governed in this case by the singly connected portions of the curve. It is easy to see that only l out of the b bonds (e.g. along an edge in figure 5) are singly connected, so that indeed one expects that $1/\nu=\ln l/\ln b$. The temperature becomes marginal for $l=1$.

We now consider the non-trivial fixed points. The coordinates of the point E are $(\tau_E^*, \tau_w=1)$. Assuming $\tau_E^*\ll 1$ we can use (3.3) to estimate its value. We obtain

$$\tanh K'=\tanh^{b-l}(bK) \qquad (\text{if } \tau_w=1), \tag{A2.7}$$

hence

$$K_E^*\simeq b^{-(b-l)/(b-l-1)}, \tag{A2.8}$$

and indeed there is a range of b and l for which $K_E^*\simeq\tau_E^*\ll 1$. To evaluate the critical exponents associated with the multicritical point E we use equations (A2.1)–(A2.4) and find that the critical exponent associated with the τ_w-direction is

$$\lambda_E=(\ln(b-l)-(b-1)K_E^*)/\ln b. \tag{A2.9}$$

In the limit $K_E^*\ll 1$, this reduces to $\lambda_E\simeq\ln(b-l)/\ln b$.

In the special case $b=l+2$, (A2.8) reduces to $K_E^*\simeq 1/b^2$. In the limit $b\gg 1$, (2.1) reduces to $D\simeq 1+\ln 4/\ln b$, and we find that

$$\lambda_E\simeq\tfrac{1}{2}(D-1). \tag{A2.10}$$

If one identifies this exponent with $1/\nu$, it is interesting to note that the result for ν differs from that for hypercubic lattices ($\nu\simeq 1/(d-1)$). However, E is a *multi*critical point (and not a regular critical one), and the lacunarity of our carpet is clearly not small (Gefen *et al* 1983b).

In the case $b=l+2>3$, the true critical properties are characterised by the point F. At this point, $K_F^*=\infty$ and

$$\tanh K_{w,F}^*=\tanh^l(2K_{w,F}^*). \tag{A2.11}$$

The exponents near F are

$$\lambda_{1,F} = (\ln l - 4K^*_{w,F})/\ln b,$$
$$\lambda_{2,F} = \ln\{l[1 - 2\tanh^2 K^*_{w,F}/(1 + \tanh^2 K^*_{w,F})]\}/\ln b. \tag{A2.12}$$

There are some more subtleties concerning the flows in the parameter space. For example, one can see (equation 3.3) that for $K = 0$ there is a fixed point on the AB axis. This point is an inflection point: stable in the direction of B and unstable in the direction of A. It is a $T = \infty$ point (corresponding to a zero correlation length) and does not represent any interesting physical behaviour. Other such points occur for the $b = l + 2$ on the AD axis, and for the 'scattered lacunarity' carpets (see text).

References

Dhar D 1980 *Pramana* **15** 545
Gefen Y, Aharony A and Mandelbrot B B 1983a *J. Phys. A: Math. Gen.* **16** 1267
Gefen Y, Aharony A, Mandelbrot B B and Kirkpatrick S 1981 *Phys. Rev. Lett.* **47** 1771
Gefen Y, Aharony A, Shapir Y and Mandelbrot B B 1984 *J. Phys. A: Math. Gen.* **17** 435
Gefen Y, Mandelbrot B B and Aharony A 1980 *Phys. Rev. Lett.* **45** 855
Gefen Y, Meir Y, Mandelbrot B B and Aharony A 1983b *Phys. Rev. Lett.* **50** 145
José J V, Kadanoff L P, Kirkpatrick S and Nelson D R 1977 *Phys. Rev.* B **16** 1217
Kadanoff L P 1976 *Ann. Phys., NY* **100** 359
Mandelbrot B B 1977 *Fractals: Form, Chance and Dimension* (New York, Oxford: Freeman)
—— 1979 *C.R. Acad. Sci., Paris* A **288** 81
—— 1982 *The Fractal Geometry of Nature* (San Francisco: Freeman)
Migdal A A 1975 *Zh. Eksp. Teor. Fiz.* **69** 1457 (1975 *Sov. Phys.-JETP* **42** 743)
Stinchcombe R B 1979 *J. Phys. C: Solid State Phys.* **12** 2625
Suzuki M 1983 *Prog. Theor. Phys.* **69** 65